

Directable Animation of Non-photorealistic Fluids

Viraj Churi, Gaurav Bhagwat and Parag Chaudhuri

Department of Computer Science and Engineering, Indian Institute of Technology Bombay, Mumbai, India

Keywords: Physically-based Fluid Simulation, Stroke-based Interface, Directable Fluids, Non-photorealistic Rendering.

Abstract: This paper presents a method to control and direct a physically-based fluid simulation with user defined strokes. Strokes are interpreted as flowlines and introduce a smooth velocity field in their vicinity that allows the fluid simulation to be easily directed by an animator. We also allow the fluid to interact with arbitrarily shaped obstacles and have variable viscosity during the simulation. The strokes can be alive for a finite duration and are registered to a timeline to give keyframing like control to the animator over the physics driven simulation.

1 INTRODUCTION

Traditionally trained animators trying to create special effects animation for fluids in two-dimensions have to be very skilled artists to capture the flow of energy that makes the movement of fluids convincing (Gilland, 2009). On the other hand, recent research in graphics (Stam, 1999; Foster and Fedkiw, 2001; Batty et al., 2007) has made physically-based simulation of fluids accessible to all. However, physics driven fluids, though mathematically realistic are often too cumbersome to control and direct for artists who cannot parse the various parameters that have to be adjusted to fine-tune the simulation. Thus, there is a need for intuitive controls for fluid animation that let artists direct the fluid behavior easily.

Our paper describes a stroke-based control method for directing the animation of fluids. We handle fluids in two-dimensions as we want to enhance and ease the work of animators trained in the 2D domain. The strokes drawn by the artist act as flowlines and the fluid is guided along these strokes. An example of these can be seen in Figure 1. The strokes are a natural interface for the artist used to sketching and drawing. Our fluid simulation is an Eulerian grid based technique that uses a combination of fluid implicit particle (FLIP) method and particle in cell (PIC) method to advect the fluid (Zhu and Bridson, 2005). We further use the variational method for the pressure solve to achieve one-way solid-fluid coupling (Batty et al., 2007). This lets us handle obstacles of arbitrary shape in the simulation.

The rest of this paper is organized as follows. We discuss related prior work and our basic fluid simula-

tion framework in Section 2. We describe our stroke-based interface for directing the fluid in Section 3, additional controls for the fluid simulation in Section 4 and our non-photorealistic renderer details in Section 5. We conclude by summarizing our results in Section 6 and the contributions of this paper, its limitations and outlining avenues for future work in Section 7.

2 BACKGROUND

We briefly review related works in grid-based fluid simulation, controlling fluid flows and non-photorealistic rendering of fluids.

2.1 Fluid Simulation

(Foster and Metaxas, 1996) introduced the first 3D grid-based solver for fluid simulation to computer graphics. This was followed by the stable fluids work of (Stam, 1999) who used Semi-Lagrangian advection to obtain unconditional stability in the simulator. (Foster and Fedkiw, 2001) used a level set for higher quality tracking of the fluid surface. Subsequently, (Zhu and Bridson, 2005) used a combination of PIC and FLIP techniques for particle advection while simulating sand as a fluid. More recent work also introduce fully implicit methods for computing two-way interactions between solids and fluids that offer better accuracy and stability (Chentanez et al., 2006; Batty et al., 2007). We are inspired by these works in creating our basic fluid simulation framework.

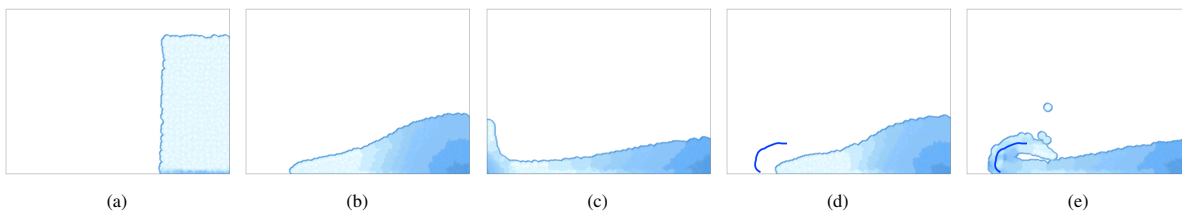


Figure 1: (a), (b) and (c) show a normal dam break simulation. (d) shows a stroke added to the frame shown in (b). This changes the resulting splash wave in the dam break simulation as shown in (e).

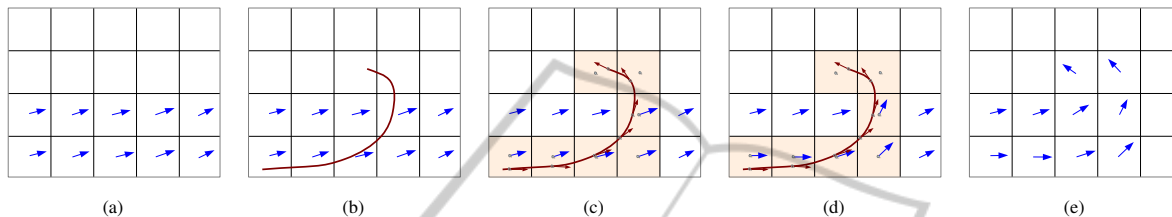


Figure 2: (a)-(b) A velocity stroke is introduced in flow (drawn in red). (c)-(d) The cells through which the stroke passes are identified and the flow velocity in those cells is changed to match the tangent vectors on the stroke. This causes the flow direction to get locally modified to match the stroke. (e) Subsequent advection steps smooth out the velocity field and spread the stroke induced velocities to nearby cells.

We solve the Navier-Stokes equations for incompressible fluid flows as given below, on a staggered grid.

$$\frac{\partial \mathbf{u}}{\partial t} + (\mathbf{u} \cdot \nabla) \mathbf{u} + \frac{1}{\rho} \nabla p = \mathbf{f} \quad (1)$$

$$\nabla \cdot \mathbf{u} = 0 \quad (2)$$

Here \mathbf{u} is the fluid velocity, ρ the fluid density, p is the pressure, and \mathbf{f} is the acceleration due to body forces such as gravity. Interested readers can refer to (Bridson, 2008) for more details on the standard grid-based fluid solver. We use the pressure solve reformulated as a kinetic energy minimization (Batty et al., 2007). This allows us to robustly handle solid-fluid interactions. We track a signed distance function by using the fast sweeping algorithm (Zhao, 2004) for computing the numerical solution of the Eikonal equation. This is used to reconstruct a smooth fluid surface at higher grid resolutions using marching squares (Lorensen and Cline, 1987). The grid resolution used for surface tracking can be controlled using the surface refinement factor that can be 1, 2 or 4 with higher numbers signifying a more refined grid.

2.2 Controlling Fluid Flows

Control of fully 3D fluid simulation was attempted early on where embedded controllers were used for altering pressure and velocity in the fluid (Foster and Metaxas, 1997). (Rasmussen et al., 2004) use particle-based controls for velocity, viscosity, level-sets and divergence. (McNamara et al., 2004) use the adjoint method to efficiently solve the non-linear

optimization problem involved in matching the control parameters to user defined keyframes. (Mihalef et al., 2004) present a slice based control mechanism to specify the keyframes of breaking waves. (Thürey et al., 2006) present a control mechanism in which control particles locally exert forces in the fluid to shape the velocity field. Even though all these controls are able to modify the fluid simulation, they are not that intuitive to specify and use. Guiding objects have also been used to control smoke simulation (Shi and Yu, 2005).

Motion trajectories and strokes have been used to control thin shell animations (Bergou et al., 2007) and character animations (Thorne et al., 2004). However, no intuitive sketch based controls for fluid simulations exist. This is the gap this work endeavors to fill.

2.3 Non-photorealistic Rendering for Fluids

Non-photorealistic rendering methods for illustrations have a rich research history in graphics (Gooch et al., 1999; Gooch and Gooch, 2001; DeCarlo et al., 2003). Cartoon style rendering for fluids has also been attempted (Eden et al., 2007). Sketch-based methods have been used to illustrate complex dynamic fluid systems (Zhu et al., 2011).

We are inspired by these methods and present our own simple non-photorealistic 2D fluid renderer that is based on metaballs (Blinn, 1982) and is implemented as a GLSL (Rost and Kessenich, 2006) shader.

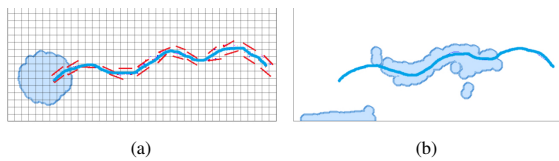


Figure 3: (a) shows a blob of fluid with the stroke. The stroke alters the local velocity field around it. The velocity vectors drawn in red are tangential to the smooth stroke. The fluid flows in the altered velocity field as is shown in (b).

3 STROKE-BASED INTERFACE

Strokes locally alter velocity field of fluid to create desired fluid flows. The strokes are drawn as smooth spline curves. These pass through the stroke points that make up a mouse or pen gesture used to draw the stroke. The grid cells through which the strokes pass are identified. The horizontal and vertical components of fluid velocity in these cells are modified so that the resultant velocity matches the tangent to the stroke at the point on the stroke that is closest to the cell center. This process is illustrated in Figure 2. The magnitude of the velocity can also be amplified to match a strength value associated with each stroke. Screenshots showing an example of this interaction in our simulator are shown in Figure 3. Here a blob of fluid is made to flow to the right by introducing a velocity stroke.

Strokes not only put restriction on direction of neighboring velocities but can also be used to control their magnitude. Velocity strokes can be of different strengths where their strength determines the magnitude of fluid velocity.

3.1 Timeline Control

The fluid simulation can only run at a timesteps at which it satisfies the CourantFriedrichsLewy (CFL) condition (Bridson, 2008) such that $\Delta t \leq \frac{\Delta x}{v_{max}}$. There is however, a difference in the simulation timesteps and the frame rate at which the animation is created. Our interface maps the simulation time to corresponding animation frames on a timeline. This timeline allows the animator to paint the strokes at a particular frame and have them active for a finite interval. Then they can be deactivated. We have divided our timeline in two parts (see Figure 4), primary and secondary. The primary timeline has step size of 75 and the secondary timeline has step size of 1. This allows for fine level keyframe control.

An example of this control can be seen in the result sequence shown in Figure 5. Here a blob of fluid



Figure 4: Primary and Secondary Timeline Controls.

splashes onto a fluid bed. The original simulation shows only a small splash. The modified simulation uses two different sets of strokes, active for different time frames, to create a bigger splash.

4 ADDITIONAL CONTROLS

In addition to the stroke based control, we allow for variable viscosity, arbitrarily shaped obstacles, sources and sinks in our simulations.

4.1 Variable Viscosity

Viscosity is usually handled in fluid simulations by implicitly solving a diffusion equation like

$$\frac{\partial \mathbf{u}}{\partial t} = \nu \nabla^2 \mathbf{u} \quad (3)$$

In addition, solution of the Navier-Stokes introduces numerical dissipation errors that visually appear as viscosity in the simulation. In our simulator, we compute fluid advection using a weighted combination of the PIC and FLIP methods. This allows for variable numerical dissipation. If even higher viscosities are desired, the coefficient of viscosity, ν , is varied and factored into the simulation by solving the diffusion equation. This combination of viscosity inducing methods is controlled by a single viscosity value. For low viscous flows the viscosity value is less than 4 and only numerical viscosity is enough. Larger values of the viscosity values increase the coefficient of viscosity.

Figure 6 shows a of frame of an animation at $t = 2$ seconds from the start of the animation where a blob of fluid is splashing into a fluid bed. In 6(a) the fluid has very low viscosity, so more fluid is displaced as the blob hits the fluid bed and so the trough is deeper. In 6(b) the trough is less deep for a more viscous fluid, while in 6(c) the viscosity is so high that the fluid blob is still falling down at this time frame.

4.2 Obstacles, Sources and Sinks

The animator can sketch arbitrary obstacles into the simulation grid that can then interact with the grid. Obstacles can be closed and open as shown in Figure 7. The simulator automatically sets appropriate boundary conditions for these obstacles.

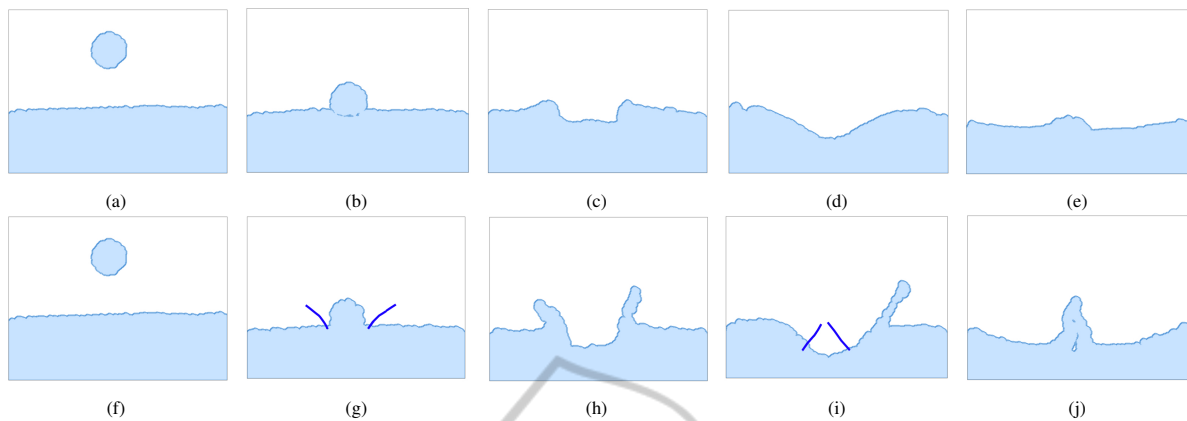


Figure 5: The top row shows the original simulation of a blob of fluid falling on a fluid bed. The bottom row shows two strokes that are active only for finite time durations during the simulation that were used to modify the animation to create a larger, more dramatic splash.



Figure 6: In (a) the viscosity value of the fluid is 1, in (b) it is 5 and in (c) it is 10.

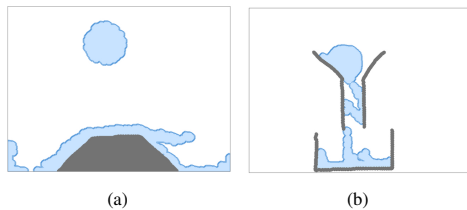


Figure 7: (a) Shows a closed obstacle on which the fluid is falling, (b) shows open obstacles used to model a funnel and vessel with the fluid interacting with them.

The simulator can also handle various kinds of fluid sources. Any arbitrary closed shape can be defined to be a body of fluid by the animator. If the shape is closed by the grid boundary on any side, it is automatically detected and the grid boundary becomes the boundary for that source object (like the fluid bed seen in Figure 5). Another type of source that can be introduced are spherical blob sources of various radii (an example of this is the drop of fluid in Figure 5). These sources can introduce fluid into the simulation at an artist specified rate, for an artist specified time.

Similar to sources, arbitrary shapes sketched by the artist can act as sinks. The boundary conditions for sinks are adjusted automatically. Sinks can also stay active for finite time durations if so desired by the animator. Figure 8 shows a bucket shaped sink absorbing the fluid blob that falls into it. Figure 9 shows an arbitrary sink

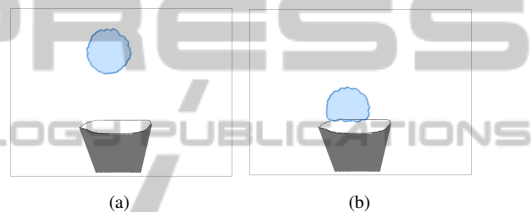


Figure 8: A bucket shaped sink absorbs the fluid blob that falls into it.

absorbing fluid flying off a ramp shaped obstacle.

5 RENDERING

We experimented with many non-photorealistic rendering techniques. Currently our rendering engine support four kinds of renderers. For fast rendering we use marker particles to track the fluid. The marker particle positions are maintained in a dynamic vertex buffer object which is used while rendering. The first kind of rendering directly renders the points, as shown in Figure 10(a). The next kind of renderer uses point sprites, where a small texture is drawn at the position of each marker particle and blended with the neighbouring sprites using alpha blending, as shown in Figure 10(b). The third kind of renderer uses a modified marching squares algorithm to fill in the triangles identified to get a solid filled fluid region (Figure 10(c)). Finally, we use a metaballs based renderer that uses the metaball potential to color fluid region (Figure 10(d)). The boundary metaballs are used to draw a smooth boundary on the fluid surface. The renderer can be swapped on the fly at runtime, as desired by an artist.

In order to further enhance the shading, we have modified the metaballs shader so that a gradient is

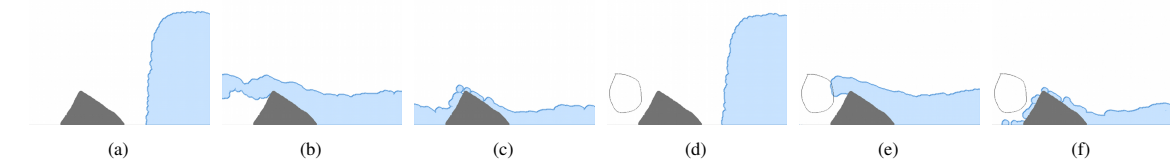


Figure 9: (a), (b) and (c) show the original simulation of a blob of fluid flying of a ramp shaped obstacle. (d), (e) and (f) show the fluid being absorbed by a sink sketched in by the artist.

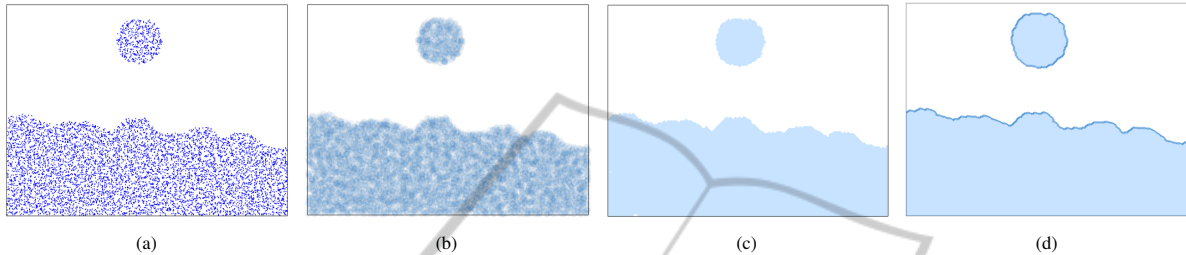


Figure 10: This image shows the various non-photorealistic renderers available in our simulator: (a) points, (b) point sprites, (c) modified marching squares and (d) metaballs. For a 30×30 grid and 16 particles per grid cell, these methods take 2.33ms, 3.72ms, 4.33ms, 7.99ms respectively to render a frame of the simulation.

produced in the fluid mass based on the displacement of the particles over a moving window of frames. Thus, the color smoothly varies from light blue in fast moving parts of the fluid to dark blue in slow moving parts, as shown in Figures 1. The window ensures that the color change is not abrupt in a particular region of the fluid. Between different regions, the colors are blended using the metaball potentials.

5.1 User Interface

The user interface consists of three main parts of which the simulation area and the settings panel can be seen in Figure 11, and a timeline control (see Figure 4). A cropped, zoomed part of the settings panel showing the controls available for strokes is also shown. The panel allows animator to tune all control parameters like stroke strength, stroke duration, source type, viscosity, obstacle type. The resulting change in the simulation can be seen in realtime in the simulation area. It also allows animator to add or remove simulation elements to simulation area.

The timeline contains a slider which allows animator to move through frames. The artist can directly draw on the simulation region to add strokes, obstacles, sources or sinks. The simulation, once configured, can also be recorded and played back.

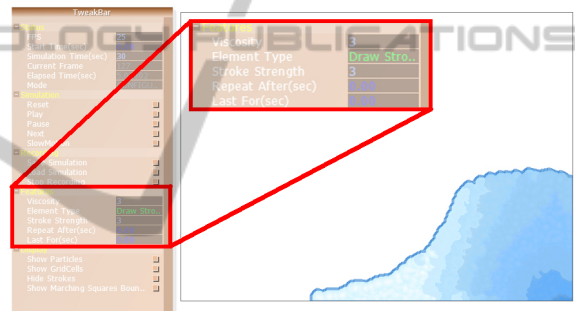


Figure 11: The user interface.

6 TIMING RESULTS

We ran our simulator on a laptop machine with an ATI Mobility Radeon HD 5470 graphics card, Intel core

i5-450M processor (3M cache, 2.40 GHz) and 4 GB RAM. Then we timed a double dam-break experiment, averaging the computation time spent for various sections of our simulator over 100 frames. The results are shown in Tables 1(a) and 1(b).

Rendering time largely depends on the rendering method used. Rendering using metaballs is computationally expensive and it takes the highest time (see Figure 10). However, it can clearly be seen that even on our modestly powered test laptop, the simulator can easily work at 25 – 30 fps for the grid resolutions reported. We have also tried our simulator on faster machines where a much higher grid resolution can be used with the simulator still working at realtime frame rates.

7 CONCLUSIONS

We have presented an efficient and intuitive stroke-based method for directing physically-based fluid

Table 1: (a) shows computation times for different grid resolutions with 16 particles per grid cell and a surface refinement factor of 2. (b) shows computation times for different number of particles per grid for a grid resolution of 40×40 and surface refinement factor of 1.

(a)				(b)			
Grid resolution	Time (ms)			Particles per grid cell	Time (ms)		
	Advection	Projection	Surface Tracking		Advection	Projection	Surface Tracking
20×20	1.56	1.36	0.22	4	2.16	4.5	0.32
30×30	3.68	2.32	0.42	8	4.1	4.48	0.30
40×40	6.08	4.96	0.78	16	6.2	4.47	0.28
50×50	10.78	7.5	1.13	32	11.52	4.32	0.32

simulations in two-dimensions. The strokes can be sketched by an artist on the simulation grid. They automatically and locally alter the velocity field and guide the fluid flow along their length. We also allow the artist to sketch arbitrary shaped obstacles, sources and sinks inside the simulation domain. All these elements can be registered to a timeline easily, allowing intuitive keyframing control to an animator. Finally, we allow for multiple non-photorealistic rendering styles for the fluid. The simulator is efficient enough to run at realtime rates and allows for all the control to be done interactively.

We would like to extend our method to take advantage of stroke dynamics and layering of intersecting strokes, which we cannot handle at present. Even though we can handle variable viscosity in our simulator, we cannot simulate multi-phase flows. We would like to extend this simulator to multi-phase flows. Our current rendering mechanism does not capture the specularity of fluids, which is frequently used to make sketched fluids look better. We would like our rendering method to be able to handle such phenomena. We would also like to experiment more with two-way solid-fluid coupling. Our current simulator already implements the variational framework that can handle two-way coupling though we have not experimented with it so far. Finally, we would like to conduct an extensive user survey to gauge the efficacy and intuitiveness of our interface for fluid control.

REFERENCES

- Batty, C., Bertails, F., and Bridson, R. (2007). A fast variational framework for accurate solid-fluid coupling. *ACM Trans. on Graphics*, 26(3):100.
- Bergou, M., Mathur, S., Wardetzky, M., and Grinspun, E. (2007). Tracks: toward directable thin shells. *ACM Trans. on Graphics*, 26(3).
- Blinn, J. F. (1982). A generalization of algebraic surface drawing. *ACM Trans. on Graphics*, 1(3):235–256.
- Bridson, R. (2008). *Fluid Simulation For Computer Graphics*. A K Peters.
- Chentanez, N., Goktekin, T. G., Feldman, B. E., and O’Brien, J. F. (2006). Simultaneous coupling of fluids and deformable bodies. In *Proceedings of the SCA*, pages 83–89.
- DeCarlo, D., Finkelstein, A., Rusinkiewicz, S., and Santella, A. (2003). Suggestive contours for conveying shape. *ACM Trans. on Graphics*, 22(3):848–855.
- Eden, A. M., Bargteil, A. W., Goktekin, T. G., Eisinger, S. B., and O’Brien, J. F. (2007). A method for cartoon-style rendering of liquid animations. In *Proceedings of Graphics Interface*, pages 51–55. ACM.
- Foster, N. and Fedkiw, R. (2001). Practical animation of liquids. In *Proceedings of SIGGRAPH*, pages 23–30.
- Foster, N. and Metaxas, D. (1996). Realistic animation of liquids. *Graphical Models and Image Processing*, 58:471–483.
- Foster, N. and Metaxas, D. (1997). Controlling fluid animation. In *Proceedings of CGI*.
- Gilland, J. (2009). *Elemental Magic, Volume 1: The Art of Special Effects Animation*. Focal Press.
- Gooch, B. and Gooch, A. (2001). *Non-Photorealistic Rendering*. AK Peters Ltd.
- Gooch, B., Sloan, P.-P. J., Gooch, A., Shirley, P., and Riesenfeld, R. (1999). Interactive technical illustration. In *Proceedings of I3D*, pages 31–38. ACM.
- Lorensen, W. E. and Cline, H. E. (1987). Marching cubes: A high resolution 3d surface construction algorithm. *Computer Graphics, SIGGRAPH 87*, 21(4).
- McNamara, A., Treuille, A., Popović, Z., and Stam, J. (2004). Fluid control using the adjoint method. In *ACM SIGGRAPH 2004 Papers*, pages 449–456. ACM.
- Mihalef, V., Metaxas, D., and Sussman, M. (2004). Animation and control of breaking waves. In *Proceedings of the SCA*, pages 315–324. Eurographics Association.
- Rasmussen, N., Enright, D., Nguyen, D., Marino, S., Sumner, N., Geiger, W., Hoon, S., and Fedkiw, R. (2004). Directable photorealistic liquids. In *Proceedings of the SCA*, pages 193–202. Eurographics Association.
- Rost, R. and Kessenich, J. (2006). *OpenGL Shading Language*. Addison-Wesley.
- Shi, L. and Yu, Y. (2005). Controllable smoke animation with guiding objects. *ACM Transactions on Graphics*, 24(1):140–164.
- Stam, J. (1999). Stable fluids. In *Proceedings of SIGGRAPH*, pages 121–128.

- Thorne, M., Burke, D., and van de Panne, M. (2004). Motion doodles: an interface for sketching character motion. *ACM Trans. on Graphics*, 23(3).
- Thürey, N., Keiser, R., Pauly, M., and Rüdè, U. (2006). Detail-preserving fluid control. In *Proceedings of the SCA*, pages 7–12. Eurographics Association.
- Zhao, H. (2004). A fast sweeping method for Eikonal equations. *Mathematics of Computation*, 74(250):603–627.
- Zhu, B., Iwata, M., Haraguchi, R., Ashihara, T., Umetani, N., Igarashi, T., and Nakazawa, K. (2011). Sketch-based dynamic illustration of fluid systems. *ACM Trans. on Graphics*, 30(6):134:1–134:8.
- Zhu, Y. and Bridson, R. (2005). Animating sand as a fluid. *ACM Trans. on Graphics*, 24:965–972.

